Title: Mapping the current distribution and predicted spread of the leishmaniosis sand fly vector in the Madrid region (Spain) based on environmental variables and expected climate change

Running Title: Mapping leishmaniosis sand fly vectors in Madrid

Authors' names and affiliations:

Rosa Gálvez [1], Miguel A. Descalzo [2], Irene Guerrero [3], Guadalupe Miró [4], Ricardo Molina [1]

[1] Servicio de Parasitología, Centro Nacional de Microbiología, Instituto de Salud Carlos III, Crtra. Majadahonda-Pozuelo s/n, 28220 Majadahonda, Madrid, Spain

[2] Unidad de Investigación, Sociedad Española de Reumatología, C/Marqués del Duero 5, 28001 Madrid, Spain

[3] Departamento de Ecología, Facultad de Ciencias, Universidad Autónoma de Madrid, C/Darwin 2, 28049 Madrid, Spain

[4] Departamento de Sanidad Animal, Facultad de Veterinaria, Universidad Complutense de Madrid, Avda. Puerta de Hierro s/n, 28040 Madrid, Spain

E-mail addresses:

Rosa Gálvez: rgalvez@isciii.es

Miguel A. Descalzo: descalzo.miguelangel@gmail.com

Irene Guerrero: ireneee@gmail.com

Guadalupe Miró: gmiro@vet.ucm.es

Ricardo Molina: rmolina@isciii.es

Keywords: *Phlebotomus perniciosus*, *Phlebotomus ariasi*, *Leishmania infantum*, climate change, GIS, spatial analysis.

Abstract

Leishmaniosis caused by *Leishmania infantum* is a widespread zoonotic disease that is endemic in the Mediterranean basin. Based on prior point abundance data for the two sand fly vectors of leishmaniosis in the Madrid region (*Phlebotomus perniciosus* and *Phlebotomus ariasi*), models were constructed to predict the spatial distribution patterns of these vectors. The models were obtained by negative binomial regression of several environmental variables and then used to map vector distributions. To validate the maps, we used serological prevalence data of *Leishmania* infection in dogs and incidence data obtained through questionnaires completed by veterinarians in the region. Seropositive dogs and veterinary clinics registering a higher incidence of canine leishmaniosis (CanL) appeared closer to our modelled vector foci. In the face of climate change, we simulated the future distributions of the sand flies for each third of the twenty first century and predicted their spread in the region.

Introduction

Leishmaniosis is a widespread endemic disease in the Mediterranean basin transmitted to humans and animals by blood-sucking phlebotomine sand flies (Killick-Kendrick, 1990). In the Madrid region, it is the most common zoonotic disease that afflicts infants (aged 0–4 years) and also frequently affects patients with HIV infection (BECM, 2005). *Phlebotomus perniciosus* and *Phlebotomus ariasi* are the proven vectors of *Leishmania infantum* in Spain (Rioux, 1986; Lucientes Curdi, 1988; Martín-Sánchez et al., 1994), *P. perniciosus* being its main vector in the Madrid region (Conesa Gallego, 1997; Gálvez et al., 2010a).

Interest in this disease has been rekindled by a proposed, yet disputed, risk of reintroduction of leishmaniosis in Europe (Dujardin et al., 2008; Ready, 2010) fuelled by the idea that climate and environmental factors determine the current geographical distribution range of its vectors. However, this zoonosis (Chargui et al., 2007; Antoniou et al., 2009; Martín-Sánchez et al., 2009; Gálvez et al., 2010b; Mazeris et al., 2010) and its vectors (Maroli et al., 2008; Gálvez et al., 2010a) have proved particularly challenging in terms of predicting their trends, and it is thought that new tools such remote sensing and geographic information systems (GIS) could help predict the spread of leishmaniosis according to changing human activities and environmental conditions (Ready, 2008). Mapping disease occurrence based on explanatory variables, or predicting its future distribution based on expected climate changes, could serve to identify potential risk areas for human infection both in space and time (Kitron, 1998; Kitron, 2000).

The first studies to apply these tools in leishmaniosis vector epidemiology emerged in the late 1990s. A model of *Phlebotomus papatasi* distribution was developed in Southwest Asia based on weather and a so-called normalized difference vegetation index (NDVI) (Cross et al., 1996). Thus, a 1–5ºC rise in ambient temperature was linked to the expansion *P. papatasi* in this region (Cross and Hyams, 1996). Also, through a logistic regression approach, a risk map was created for the presence

of *Phlebotomus orientalis* in Sudan based on soil type, mean annual daily maximum temperature and rainfall (Thomson et al., 1999).

More recently, several leishmaniosis risk maps based on environmental factors have been developed (Elnaiem et al., 2003; Gebre-Michael et al., 2004; King et al., 2004; Chamaille et al., 2010) and vector-reservoir distribution forecasts have been made under the premise of pending climate change (Peterson and Shaw, 2003; González et al., 2010).

The objectives of this study were to construct vector distribution maps for the Madrid Autonomous Region, Spain, based on environmental variables and then to project these distributions to future climate scenarios for each third of the 21st century. These maps will provide useful information on the ecology of the leishmaniosis sand fly vectors in the Madrid region on which to base the design of appropriate and focused control measures.

Materials and methods

Study site

The study was conducted under the EDEN project (www.eden-fp6project.net), whose aim is to identify and catalogue European ecosystems and environmental conditions that determine the spatial and temporal distributions and dynamics of several pathogenic agents, including *L. infantum*. The study area was the Madrid province (Fig. 1), central Spain (40°22′N and 3°43′W). The altitude of this region varies from 491–883 m in the south and centre, to 767–2400 m in its northern area. Climate and vegetation are typically Mediterranean, with hot, dry summers and maximum rainfall recorded in autumn and spring.

Entomological records

A cross-sectional survey was conducted in July 2006 and 2007 across a band spanning northeast to southwest of the Madrid region, where canine leishmaniosis (CanL) is endemic (Amela et al., 1995; Miró et al., 2007; Gálvez et al., 2010b). The area selected included a mountain range (Sistema

Central), and its foothills and plateau region. The widely-varying altitude (440 to 2414 m) of the study area determines both broad climate and vegetation ranges, influencing sand fly distributions. A description of this survey has been published elsewhere (Gálvez et al., 2010a). In brief, 123 sampling sites were set up evenly distributed across a 60-square grid (5 min each side) in the study area, and geocoded using a GPS (see Fig. 1). Moran's I test revealed no spatial autocorrelation of the entomological data (p = 0.394). Ten to twenty sticky traps (A5-size paper coated with castor oil) were set for four days at each sampling site. The traps were mainly placed inside the holes used to drain embankments or containment walls alongside roads. These sites provide the microclimate required by sand flies for diurnal rest (Rioux et al., 1982). However, since only a low number of *P. ariasi* specimens were observed the data used for model constructions were the densities of *P. pernicious* plus *P. ariasi* calculated as the number of sand flies per trap square metre recovered from the 123 sampling sites.

Environmental and meteorological variables

Using GIS software ArcGis v.9.2 (ESRI, Redlands, CA, USA), each sampling site was assigned a set of meteorological and environmental variables including: mean rainfall recorded over the four seasons of a year; minimum, maximum and mean temperatures for the four seasons; altitude; aspect; land cover; distance to urban settlement; distance to nearest livestock farm (cows, goats, pigs, horses and sheep) and distance to nearest poultry farm (quails, pheasants, chickens, geese, pigeons, ducks, turkeys, partridges, guinea fowl or ratites).

Daily temperature and precipitation data were provided by the Spanish Meteorological Agency (AEMet). Each sampling site was assigned data from the closest meteorological station in the study area (n=38) using the spatial join-and-relate tool of the GIS software. The maximum distance between a sampling site and the nearest meteorological station was less than 5 km. Temperature and precipitation values were those recorded from September to November, December to February, and

March to May of the year before the sampling date, and during the summer (June to August) when the field work was conducted. Using the Spatial Analyst application (SAA) of the GIS software, we then extracted corresponding values for the topographical variables (altitude and aspect) from a Shuttle Radar Topography Mission (SRTM) 90 m resolution digital elevation model (DEM) " Copyright DLR <2000>". A 300 m resolution land cover layer based on MERIS satellite imagery from January 2005 to June 2006 provided by the European space agency (ESA) was used to define the following land use categories: cultivated areas, forest and shrubland, sparse vegetation, urban areas and water bodies. Through SAA, land cover values for each sampling site were obtained by: (a) corresponding land cover extractions (model 1); or (b) percentages of land cover categories in a 250 m and 500 m buffer zone around each sampling site (model 2), a distance equivalent to estimated reach of sand fly flight (Rioux et al., 1979; Killick-Kendrick et al., 1984). Using the SAA tool of the GIS software, a 250 m resolution raster was created by calculating the straight-line distance from each cell to the urban settlement feature layer of the Madrid region. From each record, a corresponding value was extracted from this raster layer. Data for the 11,238 livestock and 1,142 poultry farms in the study area were supplied by the Spanish Ministry of the Environment and Rural and Marine Affairs. Each sampling site was also assigned a value corresponding to its distance from the closest livestock and poultry farm using the spatial join-and-relate tool of the GIS software.

Modelling sand fly vector distributions

Two statistical approaches were used to predict the geographic distributions of the leishmaniosis vectors in the Madrid region. These models estimated vector densities as a count response regression, in which environmental and meteorological factors were used as explanatory variables. Both models assumed an over-dispersed Poisson distribution of the data, which means that a negative binomial distribution was used instead of a Poisson distribution (Hilbe, 2007). The first

model included corresponding land cover extractions, while the second included percentages of land cover categories in a buffer zone. The remaining environmental and meteorological variables were the same in both models. The model building strategy was: first, all factors were analyzed by bivariate analysis and then, starting with all variables showing a p-value lower than 0.2 in the bivariate analysis, multivariate backward stepwise regression was conducted. The likelihood ratio test was used to compare nested models and the Bayesian information criterion (BIC) was used to select the best models. To assess the predictive performance of the model, bootstrapping was performed with a 1,000 replicates to predict point-values and class values (using Jenks' natural breaks classification scheme) (Jenks and Caspall, 1971) of apparent density (AD): number of sand flies per trap square metre. R-squared was used to compare observed versus expected point values and the kappa statistic was then used to assess agreement after classifying the data in 5 groups. All statistical analyses were performed using Stata v.10.1 software (StataCorp LP, College Station, Texas, USA). The level of significance was set at a p-value lower than 0.05.

Predictive maps for the Madrid region were drawn using the Raster Calculator of the GIS software through modelling on chartable raster layers. Models were constructed based on distance (250 m resolution straight-line distances), DEM (90 m resolution), land use (500 m resolution forest and shrubland percentage) and climatic layers (200 m resolution rainfall and temperature). The latter were created and provided free by the Autonomous University of Barcelona at http://opengis.uab.es/wms/iberia/index.htm.

Validating predictive maps

Over the years 2006 and 2007 in a survey of 1,076 dogs from 32 villages in the Madrid region, anti *Leishmania* specific antibodies were detected in 87 dogs using an indirect immunofluorescence antibody test (IFAT) and a cut-off of 1/80 (Gálvez et al., 2010b). Moreover, 760 questionnaires designed for the EDEN-LEI project were sent to veterinary practitioners in December 2006 and

March 2007. The questionnaire was designed to obtain data regarding the number of dogs examined in the past year at the veterinary clinic and the number of probable cases of CanL. 166 of these questionnaires were completed and returned, and the proportion of infected or sick dogs was calculated for each clinic. The locations of individual dogs and veterinary clinics were geocoded using the Geocoding tool of the GIS software on a street map layer for the Madrid province updated in 2004.

Predictive sand fly distributions were categorized into 5 classes using Jenks' natural breaks classification scheme. Outlier values of sand fly distribution were classified as "not present" for the extreme minimum (1% of cases) and "maximum density" for the extreme maximum (1% of cases). Distances from dog reservoirs (1,076) and clinics (166) to each one of the classes were assigned using the spatial join-and-relate tool of the GIS software. Associations between infected dogs or proportions of infected dogs and distance to vector foci (or classes) were used to validate predictive maps.

Climate projections

Future climate projections were estimated from the seasonal mean temperature and precipitation data expected for the centre of the Iberian Peninsula in each third of the 21st century (de Castro et al., 2005). We considered the results provided by an ensemble of six models (CCGM, CSIRO, HadCM3, NIES2, ECHAM4 and GFDL) called Atmosphere-Ocean General Circulation Model (AOGCM) using the two most used emission scenarios A2 and B2 (IPCC, 2007). In A2, greenhouse gas emissions and sulphate aerosols are predicted to rise at a more rapid rate than in B2. Maps of future sand fly distributions on the premise of the climate change scenarios were modelled, incorporating future climate projections.

Results

Model outputs under current climate

Using two different but similar models, sand fly distributions were estimated by negative binomial regression using the data collected from the sampling sites.

Model 1 revealed that the variables distance to urban settlement (US), altitude and distance to nearest livestock farm (NLF) had an effect on vector densities (Table 1). The apparent density (AD) throughout the Madrid region was predicted by the equation:

$$AD = e^{(4.67183 + \text{Distance to US} \times 0.05198 + \text{Altitude} \times (-0.18247) + \text{Distance to NLF} \times (-0.4169))} \quad \text{Equation 1}$$

Model 2 indicated that the AD for the Madrid area could be predicted from a linear combination of the variables (Table 1): mean spring rainfall, mean autumn temperature, distance to US, percentage forest and shrubland in a 500 m buffer and distance to NLF, according to the equation:

$$AD = e^{(0.2654961 + \text{Spring rainfall} \times (-0.342962) + \text{Autumn temperature} \times 0.2591498 + \text{Distance to US} \times 0.00546671 + \%\text{Forest \& shrubland} \times (-0.7546061) + \text{Distance to NLF} \times (-0.4010263))} \quad \text{Equation 2}$$

Percentage forest and shrubland in a 500 m buffer, distance to nearest livestock farm, mean spring rainfall and altitude were negatively correlated with vector density, such that the higher the value of the factor (for example, the greater the distance to the nearest farm), the lower the density of the vectors. In contrast, mean autumn temperature and distance to urban settlement were positively correlated with vector density.

The exponentiated coefficients of the models are interpreted as sand fly vector density ratios (DR), which means that for every unit increase in the value of a factor (for example a one degree increase in mean autumn temperature), the vector density will increase by 25.9%.

Bootstrap values indicated that model 2 [R-squared=0.45; 95%CI (0.23–0.73)] was better at predicting point-values of AD than model 1 [R-squared = 0.37; 95% CI (0.19–0.71)]. Moreover, for model 2, observed agreement (79.7%) was significant (p = 0.0068), though expected agreement was also high (75.3%) when AD was classified into 5 classes using Jenks' natural breaks scheme.

We then constructed two 500 m resolution maps to predict the distributions of the leishmaniosis vectors in the Madrid region, using the environmental and meteorological risk factors identified in the models mentioned above. As shown in Fig. 2, the maps are fairly similar, although class values are slightly lower for model 1. High vector density areas can be seen in the south-east, south-west and centre of the Madrid region.

The two maps were validated by considering means of distances from individual dogs and veterinary clinics to each of the 5 different classes used to classify vector density. Since the results for both maps were similar, only those for model 2 are shown. Thus, dogs seropositive for CanL appeared closer ($p = 0.048$) to the zones of higher ADs (>79.55). The clinics reporting a higher incidence of CanL were also correlated ($p = 0.0308$) with the areas showing higher ADs (>79.55). As no association was found below this point, it may be stated that, according to model 2, areas with an AD greater than 79.55 are considered vector foci.

Predicted climate change effects

Through the six-model AOGCM ensemble, the predicted spread of AD was computed using the GIS software for each third of the 21st century under the two emission scenarios A2 and B2 (Table 2). Distribution and abundance vector forecasts were based only on climate shifts. Although other risk factors such as land use will obviously intervene, these are hard to predict with much confidence and the complex methods needed are beyond the scope of this study. Thus, although both models behaved similarly, only model 2 was used for the simulations since it includes variables based on climate. Simulated climate change predicted increased vector densities and affected areas (Fig. 3). The risk of spread is greater for the A2 than the B2 scenario and is especially high for the last part of the century compared to the current situation.

Discussion

To understand sand fly vectorial capacities, knowledge of their specific environmental requirements is essential. In this study, we explored the effects of chartable environmental and meteorological variables on vector densities to map their predicted current distribution in the Madrid region. The environmental and meteorological factors considered have been previously observed to affect vector distributions in this region (Gálvez et al., 2010a).

Model 1 was based on altitude rather than the land cover (percentage forest and shrubland) and meteorological variables used in model 2, indicating that altitude encompasses the effects of both climate and vegetation factors. Thus, model 2 may be considered more appropriate from an ecological standpoint, stressing the importance of taking into account vector spread using buffers (model 2) instead of point extractions (model 1). Although our models could be improved, environmental and meteorological factors emerged as decisive for modelling sand fly distributions. Since we did not include animal reservoir, *Leishmania* parasite, and/or leishmaniosis disease data in the models, the maps do not reflect the distribution of the disease. Notwithstanding, in a recent study the average prevalence of CanL was estimated to have increased from 5.25% to 8.1% in the last 15 years among the non-stray dogs in the Madrid region (Gálvez et al., 2010b). Moreover, the spatial association detected between infected dogs and the proportion of infected dogs to modelled vector foci determines that vector density could be used as an indicator of infection risk in a given area.

The percentage forest and shrubland around each site was the factor least correlated with vector densities, probably because these sand flies seem to show a preference for more anthropogenic environments. Conversely, higher vector densities were recorded at sites far from very urban settlements. Thus, it seems that a balance between anthropogenic (urban settlements) and wild (forest and shrubland) environments (e.g., residential areas) maintains these parasite vectors in peak condition. A nearby livestock farm usually leads to increased vector densities. In a study performed

in Brazil, the proximity of livestock, pigpens or hen houses significantly increased the risk of CanL (Moreira et al., 2003). In the present study, mean rainfall recorded in the preceding spring was negatively correlated with vector densities probably because, as other authors have suggested, high rainfall conditions could damage larval habitat and reduce phlebotomine abundances (Ghosh et al., 1999; Rossi et al., 2008). Higher mean temperatures in the preceding autumn gave rise to higher vector densities. Thus, mild weather in the autumn could delay the beginning of diapause, increasing the larval population that reaches the fourth instar. Altitude was negatively correlated with vector densities. As altitude increases, vegetation changes, temperature decreases (according to the thermal gradient at a rate of –0.6ºC per 100 m) and precipitation increases. Thus, an increased altitude will provide a more hostile environment for sand fly survival. In Sudan, it has been determined through map modelling that average rainfall and altitude are the best predictors of the incidence of leishmaniosis (Elnaiem et al., 2003).

In recent years, several leishmaniosis risk maps have been produced, based on environmental factors such as altitude and rainfall (Elnaiem et al., 2003), NDVI and land surface temperature (LST) (Gebre-Michael et al., 2004) or altitude and land use (King et al., 2004). Recently, the first risk map for CanL in France was created, based on environmental variables and human-dog densities (Chamaille et al., 2010).

In central Spain (mainly in the Madrid region), vector densities a few years ago were significantly higher than densities reported 17 years earlier (Gálvez et al., 2010a). In Spain, the past 30 years have definitely seen a generalised temperature rise, whereas precipitation has shown no clearly defined trend (de Castro et al., 2005; Bladé et al., 2010). This suggests that vector densities could continue to rise, and by examining the effects of climate change we should be able to confirm this trend.

The climate change simulated returned enhanced vector densities and expansion of their distribution range. The risk of spread was greater for the A2 scenario than for the B2 scenario, because of the higher estimated anthropogenic emissions of the former. The expansion of suitable sand fly habitats was predicted. In addition, simulated climate change predicted a 3-fold increase in apparent vector densities over the period 2070–2100 under scenario A2, compared to the current situation. Since vector, host and pathogen populations intersect within a permissive environment to enable pathogen transmission (Reisen, 2010), if conditions for one of these, such as the vector, improve as predicted by our data, this could lead to improved disease transmission in the region. Predicted leishmaniosis vector-reservoir spread under the premise of climate change (IPCC, 2007) has been reported for three *Lutzomyia* species in south Brazil for 2040–2069 (Peterson and Shaw, 2003), and northwards for two *Lutzomyia* and four reservoir species in the US in 2020, 2050 and 2080 (González et al., 2010). Global change, including the development of new areas, changing agricultural practices, changing land uses and climate change, contributes to the spread of leishmaniosis (Ready, 2008). In the interest of public health, there is a need for research targeted at the prediction, prevention, diagnosis, treatment, and prevention of leishmaniosis. Information on the prevalence and geographical distribution of infection is required for the installation of control measures and their surveillance thereafter. GIS and remote sensing technology are useful tools for analysing spatial and temporal landscape features that will help identify target populations and also serve to address the behaviour of the disease and its vectors so that effective control measurements may be implemented.

The vector distribution maps and predictive models established in this study provide information on the ecology of the leishmaniosis vectors in the Madrid region, on which to base appropriate and focused control measures against human and canine leishmaniosis infection.

Acknowledgements

The authors thank the Spanish Ministry of the Environment and Rural and Marine Affairs for provided meteorological data through the Spanish Meteorological Agency (AEMet) and data on the livestock and poultry farms registered in the study area. We also thank the Madrid Veterinary Association (AMVAC) for sending the questionnaires to its members and veterinarians who kindly answered the questionaires. We thank Paul Ready, Jonathan Cox and Clive Davies for formulating the general approach to EDEN-LEI project and advising on some practical aspects of samplings and analysis. Jorge Barón helped with the design of the figures.

This work was supported by the Instituto de Salud Carlos III and the EU FP6 project "EDEN" (GOCE-2003-010284), Subproject EDEN-LEI, catalogued by the EDEN Steering Committee as EDEN0233 (www.eden-fp6project.net). The contents of this manuscript are the sole responsibility of the authors and do not necessarily reflect the views of the European Commission.

Disclosure statement

No competing financial interests exist

References

Amela C, Méndez I, Torcal JM, Medina G, et al. Epidemiology of canine leishmaniasis in the Madrid region, Spain. Eur J Epidemiol 1995; 11:157-161.

Antoniou M, Messaritakis I, Christodoulou V, Ascoksilaki I, et al. Increasing incidence of zoonotic visceral leishmaniasis on Crete, Greece. Emerg Infect Dis 2009; 15:932-934.

BECM. Zoonosis. Comunidad de Madrid, años 2002 - 2004. Boletín Epidemiológico de la Comunidad de Madrid 2005; 11:47-77.

Bladé I, Cacho I, Castro-Díez Y, Gomis D, et al. Clima en España: pasado, presente y futuro. Informe de evaluación del cambio climático regional, 2010 Red Temática CLIVAR-España

Conesa Gallego E, Romera Lozano, H & Martinez Ortega, E. Estudio de las poblaciones de flebotomos (Diptera, Psychodidae) de la Comunidad de Madrid (España). Anales de Biología 1997; 22:43-50.

Cross ER, Hyams KC. The potential effect of global warming on the geographic and seasonal distribution of Phlebotomus papatasi in southwest Asia. Environ Health Perspect 1996; 104:724-727.

Cross ER, Newcomb WW, Tucker CJ. Use of weather data and remote sensing to predict the geographic and seasonal distribution of Phlebotomus papatasi in southwest Asia. Am J Trop Med Hyg 1996; 54:530-536.

Chamaille L, Tran A, Meunier A, Bourdoiseau G, et al. Environmental risk mapping of canine leishmaniasis in France. Parasit Vectors 2010; 3:31.

Chargui N, Haouas N, Gorcii M, Akrout Messaidi F, et al. Increase of canine leishmaniasis in a previously low-endemicity area in Tunisia. Parasite 2007; 14:247-251.

de Castro M, Martín-Vide J, Alonso S. The climate of Spain: past, present and scenarios for the 21st century. A preliminary assessment of the impacts in Spain due to the effect of climate change. 2005, Ministry of Environment**,** Spain.

Dujardin JC, Campino L, Cañavate C, Dedet JP, et al. Spread of vector-borne diseases and neglect of Leishmaniasis, Europe. Emerg Infect Dis 2008; 14:1013-1018.

Elnaiem DE, Schorscher J, Bendall A, Obsomer V, et al. Risk mapping of visceral leishmaniasis: the role of local variation in rainfall and altitude on the presence and incidence of kala-azar in eastern Sudan. Am J Trop Med Hyg 2003; 68:10-17.

Gálvez R, Descalzo MA, Miró G, Jiménez MI, et al. Seasonal trends and spatial relations between environmental/meteorological factors and leishmaniosis sand fly vector abundances in Central Spain. Acta Trop 2010a; 115:95-102.

Gálvez R, Miró G, Descalzo MA, Nieto J, et al. Emerging trends in the seroprevalence of canine leishmaniosis in the Madrid region (central Spain). Vet Parasitol 2010b; 169:327-334.

Gebre-Michael T, Malone JB, Balkew M, Ali A, et al. Mapping the potential distribution of Phlebotomus martini and P. orientalis (Diptera: Psychodidae), vectors of kala-azar in East Africa by use of geographic information systems. Acta Trop 2004; 90:73-86.

Ghosh K, Mukhopadhyay J, Desai MM, Senroy S, et al. Population ecology of Phlebotomus argentipes (Diptera: Psychodidae) in West Bengal, India. J Med Entomol 1999; 36:588-594.

González C, Wang O, Strutz SE, González-Salazar C, et al. Climate change and risk of leishmaniasis in North America: predictions from ecological niche models of vector and reservoir species. PLoS Negl Trop Dis 2010; 4:e585.

Hilbe JM. Negative binomial regression, 2007 Cambridge University Press, New York, Cambridge, United Kingdon.

IPCC. Climate Change 2007: The Physical Science Basis. Contribution of Working Group I to the Fourth Assessment Report of the Intergovernmental Panel on Climate Change, 2007, Cambridge University Press, Cambridge, United Kingdom and New York, NY, USA. In: Solomon S, Qin D, Manning M, Chen Z, et al, ed.

Jenks G, Caspall F. Error on chloropletic maps: definition, measurement, reduction. Ann Assoc Am Geogr 1971; 61:217-244.

Killick-Kendrick R. Phlebotomine vectors of the leishmaniases: a review. Med Vet Entomol 1990; 4:1-24.

Killick-Kendrick R, Rioux JA, Bailly M, Guy MW, et al. Ecology of leishmaniasis in the south of France. 20. Dispersal of Phlebotomus ariasi Tonnoir, 1921 as a factor in the spread of visceral leishmaniasis in the Cevennes. Ann Parasitol Hum Comp 1984; 59:555-572.

King RJ, Campbell-Lendrum DH, Davies CR. Predicting geographic variation in cutaneous leishmaniasis, Colombia. Emerg Infect Dis 2004; 10:598-607.

Kitron U. Landscape ecology and epidemiology of vector-borne diseases: tools for spatial analysis. J Med Entomol 1998; 35:435-445.

Kitron U. Risk maps: transmission and burden of vector-borne diseases. Parasitol Today 2000; 16:324-325.

Lucientes Curdi J, Sánchez Acedo, C., Castillo Hernández, J.A., Estrada Peña, A. Sobre la infección natural por *Leishmania* en *Phlebotomus perniciosus* Newstead, 1911 y *Phlebotomus ariasi* Tonnoir, 1921, en el foco de leishmaniosis de Zaragoza. Rev Iber Parasitol 1988; 48:7-8.

Maroli M, Rossi L, Baldelli R, Capelli G, et al. The northward spread of leishmaniasis in Italy: evidence from retrospective and ongoing studies on the canine reservoir and phlebotomine vectors. Trop Med Int Health 2008; 13:256-264.

Martín-Sánchez J, Guilvard E, Acedo-Sánchez C, Wolf-Echeverri M, et al. Phlebotomus perniciosus Newstead, 1911, infection by various zymodemes of the Leishmania infantum complex in the Granada province (southern Spain). Int J Parasitol 1994; 24:405-408.

Martín-Sánchez J, Morales-Yuste M, Acedo-Sánchez C, Barón S, et al. Canine leishmaniasis in southeastern Spain. Emerg Infect Dis 2009; 15:795-798.

Mazeris A, Soteriadou K, Dedet JP, Haralambous C, et al. Leishmaniases and the Cyprus Paradox. Am J Trop Med Hyg 2010; 82:441-448.

Miró G, Montoya A, Mateo M, Alonso A, et al. A leishmaniosis surveillance system among stray dogs in the region of Madrid: ten years of serodiagnosis (1996-2006). Parasitol Res 2007; 101:253-257.

Moreira ED, Jr., de Souza VM, Sreenivasan M, Lopes NL, et al. Peridomestic risk factors for canine leishmaniasis in urban dwellings: new findings from a prospective study in Brazil. Am J Trop Med Hyg 2003; 69:393-397.

Peterson AT, Shaw J. Lutzomyia vectors for cutaneous leishmaniasis in Southern Brazil: ecological niche models, predicted geographic distributions, and climate change effects. Int J Parasitol 2003; 33:919-931.

Ready PD. Leishmaniasis emergence and climate change. Rev Sci Tech 2008; 27:399-412.

Ready PD. Leishmaniasis emergence in Europe. Euro Surveill 2010; 15:19505.

Reisen WK. Landscape epidemiology of vector-borne diseases. Annu Rev Entomol 2010; 55:461-483.

Rioux JA, Guilvard, E., Gallego, J., Moreno G., Pratlong, F., Portús, M., Rispail, P., Gallego, M., Bastien, P. *Phlebotomus ariasi* Tonnoir, 1921 *et Phlebotomus perniciosus* Newstead, 1911 vecteurs du complexe *Leishmania infantum* dans un même foyer: Infestations par deux zymodèmes syntopiques. A propos d´une enquête en Catalogne (Espagne). In: *Leishmania*. Taxonomie et Phylogenèse. Applications Éco-Épidemiologiques (IMEEE, ed), 1986, 439-444**,** Montpellier.

Rioux JA, Killick-Kendrick R, Leaney AJ, Turner DP, et al. [Ecology of leishmaniasis in the south of France. -- 12. Horizontal dispersion of Phlebotomus ariasi Tonnoir, 1921. Preliminary experiments (author's transl)]. Ann Parasitol Hum Comp 1979; 54:673-682.

Rioux JA, Perieres J, Killick-Kendrick R, Lanotte G, et al. [Ecology of leishmaniasis in south France. 17. Sampling of Phlebotomus by the method of adhesive traps. Comparison with the technic of capture on human bait]. Ann Parasitol Hum Comp 1982; 57:631-635.

Rossi E, Bongiorno G, Ciolli E, Di Muccio T, et al. Seasonal phenology, host-blood feeding preferences and natural Leishmania infection of Phlebotomus perniciosus (Diptera, Psychodidae)

in a high-endemic focus of canine leishmaniasis in Rome province, Italy. Acta Trop 2008; 105:158-165.

Thomson MC, Elnaiem DA, Ashford RW, Connor SJ. Towards a kala azar risk map for Sudan: mapping the potential distribution of Phlebotomus orientalis using digital data of environmental variables. Trop Med Int Health 1999; 4:105-113.

Reprint address

Dr. Ricardo Molina

Instituto de Salud Carlos III

Centro Nacional de Microbiología

Servicio de Parasitología

Ctra. Majadahonda-Pozuelo s/n

28220 Majadahonda – Madrid

Spain

E-mail: rmolina@isciii.es

Legends to figures

Figure 1. Geocoded locations of dogs, vectors, meteorological stations and veterinary clinics.

Figure 2. Spatial distributions of the leishmaniosis vectors predicted by models 1 and 2.

Figure 3. Predicted future distributions by the AOGCM ensemble of the leishmaniosis vectors for each third of the 21st century under the A2 emission scenario: **A**: 2010-2040; **B**: 2040-2070; **C**: 2070-2100; and B2 emission scenario: **D**: 2010-2040; **E**: 2040-2070; **F**: 2070-2100.

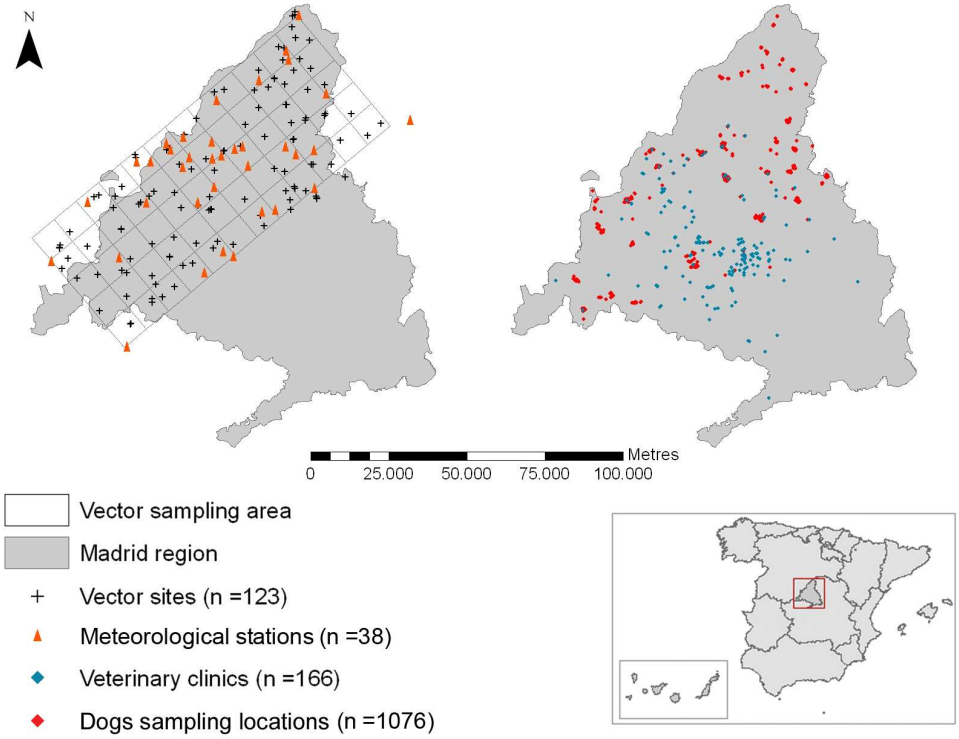

Geocoded locations of dogs, vectors, meteorological stations and veterinary clinics.
140x106mm (300 x 300 DPI)

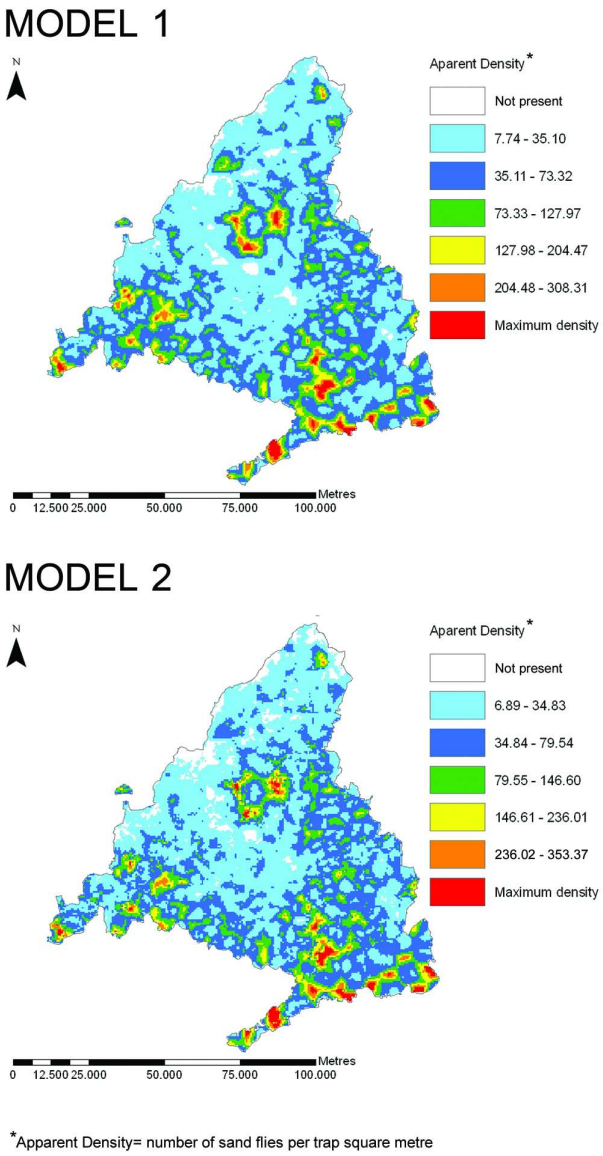

Spatial distributions of the leishmaniosis vectors predicted by models 1 and 2
90x169mm (300 x 300 DPI)

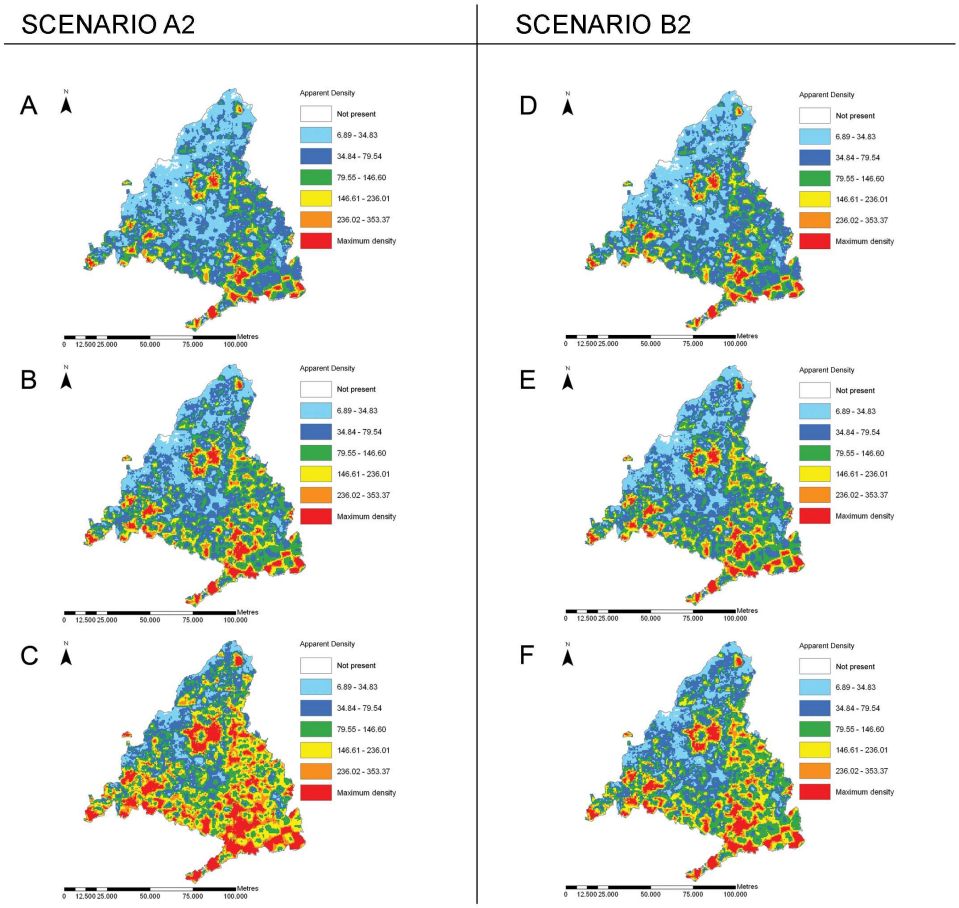

Predicted future distributions by the AOGCM ensemble of the leishmaniosis vectors for each third of the 21st century under the A2 emission scenario: A: 2010-2040; B: 2040-2070; C: 2070-2100; and B2 emission scenario: D: 2010-2040; E: 2040-2070; F: 2070-2100
189x180mm (300 x 300 DPI)

Table 1. Multivariate factors correlated with *P. perniciosus* and *P. ariasi* densities in models 1 and 2

Model	Predictor	Multivariate DR (95% CI)	p value	Coeficient	Constant
1	Distance to US (hm)	1.053 (1.020–1.088)	0.0010	0.05198	4.67183
	Altitude (hm)	0.833 (0.766–0.906)	0.0000	–0.18247	
	Distance to NLF (km)	0.659 (0.492–0.883)	0.0050	–0.41696	
	Spring mean rainfall (mm)	0.710 (0.530–0.949)	0.0210	–0.342962	
2	Autumn mean temperature (ºC)	1.296 (1.147–1.464)	0.0000	0.2591498	0.2654961
	Distance to US (hm)	1.056 (1.023–1.090)	0.0010	0.0546671	
	% Forest & shrubland in a 500 m buffer	0.470 (0.228–0.969)	0.0410	–0.7546061	
	Distance to NLF (km)	0.670 (0.501–0.895)	0.0070	–0.4010263	

DR, Sand fly vector density ratio; CI, Confidence interval; US, Urban settlement; NLF, Nearest livestock farm; hm, Hectometres; km, Kilometres; mm, Millimetres; ºC, Degrees Celsius.

Table 2. Changes in mean autumn temperature (ºC) and mean spring rainfall (mm/day) projected by the AOGCM ensemble for the central Iberian Peninsula

Period	Scenario	Designation in Fig. 3	Mean autumn temperature rise (ºC)	Mean spring rainfall reduction (mm/day)
2010-2040	A2	A	1.4	0.21
	B2	D	1.6	0.25
2040-2070	A2	B	2.9	0.28
	B2	E	2.6	0.33
2070-2100	A2	C	4.9	0.53
	B2	F	3.7	0.30

mm, Millimetres; ºC, Degrees Celsius; AOGCM, Atmosphere-Ocean General Circulation Model